

SEASONAL VARIATIONS OF VEGETATION COVER SCATTERING PROPERTIES

Liudmila N. Zakharova, Alexander I. Zakharov

Kotelnikov Institute of Radioengineering and Electronics of RAS, Fryazino branch, <http://fire.relarn.ru>
Fryazino 141190, Moscow Region, Russian Federation

zakharova@ire.rssi.ru, aizakhar@ire.rssi.ru

Abstract. In our paper Transbaikalian test sites were used to demonstrate the dependence of the vegetation covers radiophysical properties from environmental conditions, and air temperature first of all. The data of Japanese spaceborne polarimetric radar PALSAR acquired at various combinations of signal polarization on receive/transmit over several years were used to measure scattering properties of underlying covers at 8 test sites and to estimate input of various scattering mechanisms in radar signal backscatter. It was discovered that at low negative temperatures in winter the normalized radar cross-section level of vegetation covers decreases rapidly for all the signal polarization combinations. The greatest fall, up to 12 dB, is observed at cross polarization, and it is about 7-8 dB for copolarized signals. Polarimetric decomposition of scattering matrix shows the specificity of the scattering mechanisms temporal behavior depending on the air temperature. If surface scattering with low entropy is typical for vegetation-free soils all the year around, the dipole scattering mechanism of forests in summer is almost completely replaced by the class of surface scattering with moderate entropy in winter. Such a specificity of annual behavior of the sounding media scattering properties may affect the efficiency of automated methods of the underlying covers classification and an accuracy of their biophysical characteristics measurements.

Keywords: synthetic aperture radar, normalized radar cross-section, polarimetric decompositions, vegetation classification

UDC 528.8.044.2, 537.871.5

Bibliography - 13 references

Received 02.04.2019, accepted 17.04.2019

RENSIT, 2019, 11(1):49-56

DOI: 10.17725/rensit.2019.11.049

CONTENTS

1. INTRODUCTION (49)
 2. TEST SITES (50)
 3. NRCS VALUES FOR DIFFERENT COMBINATIONS OF TRANSMIT/RECEIVE SIGNAL POLARIZATION (50)
 4. POLARIMETRIC CLASSIFICATIONS AND THEIR DYNAMICS DURING THE YEAR (52)
 5. CONCLUSION (55)
- REFERENCES (55)

1. INTRODUCTION

Radar observations of the Earth from space can provide a unique information about the planet state, its biological diversity, natural resources and ecological situation in the area of observations. Vegetation is one of the principal elements of biosphere, and it is of paramount importance at the phase of design

of synthetic aperture radar and discussing its parameters, as well as later at the stage of satellite acquisition planning and observations. The potential of radar for the vegetation classification, estimation of the trees height and age, biomass evaluation, and forest borders detection as well as forest health monitoring is widely recognized.

Normalized radar cross-section (NRCS) is a radiophysical parameter which is traditionally used for the thematic mapping of forests. Regression analysis of NRCS and direct ground measurements of forest characteristics show a good correlation, and such an analysis of coniferous forests show the most impressive results [1, 2]. Multi-channel approach improves the efficiency of a forest mapping problem solution, specifically

a multi-temporal analysis [3, 4], multi-frequency observations [5–7], interferometric [8] and polarimetric [9] imaging, and also their combinations, e.g., polarimetric interferometry [10, 11]. Polarimetric observations are especially informative due to polarimetric target decomposition methods [12, 13], that allows identifying and evaluating contribution of different scattering mechanisms. Radiophysical properties of vegetation essentially depend on the environment state, e.g. precipitation and air/soil/vegetation temperature. Variations of scattering properties of forests for different signal polarizations are examined in [4]. This paper aims at study of Transbaikalia forests scattering properties variations, and, first of all, their scattering mechanisms in different seasons of year.

2. TEST SITES

Our test sites are located in the Selenga River delta in Transbaikalia region. For the estimation of natural covers NRCS values we took 8 relatively homogenous patches on the surface that have small areas from 0.3 to 1 km² (see **Table 1**). Three of them are in forested areas: two located on the flatland (in the **Fig. 1** marked as 1: coniferous forest near Dubinino settlement and 2: mixed forest near Istomino settlement), as well as mountainous forest 3 on the spur of Hamar-Daban massif (the dominating tree species are fir and cedar). Two next test sites are in between the delta arms: area 4 has some spots of shrubs on it, and 5 is covered by grass only. Other test sites are: two

agricultural fields 6 and 7, and grassland 8 not far from an unkept irrigation system.

We performed the measurements using 13 quad-polarization L-band scenes acquired by L-band PALSAR instrument in 2006-2008, in different months of a year and under different weather conditions.

3. NRCS VALUES FOR DIFFERENT COMBINATIONS OF TRANSMIT/RECEIVE SIGNAL POLARIZATION

Under freezing conditions (air temperature below zero) NRCS values of forest in L-band can decrease by 3 dB in comparison with warmer seasons [4]. This fact is associated with changes of dielectric constant of a scattering surface under different weather/season conditions. For the series of polarimetric radar images we compared mean values of NRCS for three forest test sites, see results in the Fig. 1.

For all the three combinations of transmit/receive polarization and for all forest test sites one can note two minima corresponding to two frosty days November 30, 2006, and November 16, 2007. NRCS demonstrates the most pronounced decrease for cross polarization, there the variation reaches 12 dB, whereas co-polarized NRCS shows the variation less than 7-8 dB.

It is worth noting that mountainous forest has NRCS values which are less than one that flatland forests have, especially in HH polarization. In addition, co-polarized plot for the mountainous forest shows a monotone decrease from June-July to

Table

Test sites

No.	Location and name	Area, km ²	Vegetation
1	near Dubinino (forest D)	1	coniferous forest (pine, fir)
2	near Istomino (forest I)	1	mixed forest (birch, aspen, pine, fir))
3	in mountains (Hamar-Daban)	1	coniferous forest (fir)
4	within Selenga delta (Delta-1)	0.6	spots of shrub
5	within Selenga delta (Delta-2)	0.3	grass
6	near Dubinino (field D)	0.5	cultivated field
7	near Istomino (field I)	0.8	cultivated field
8	near Istomino (grassland)	1	grass

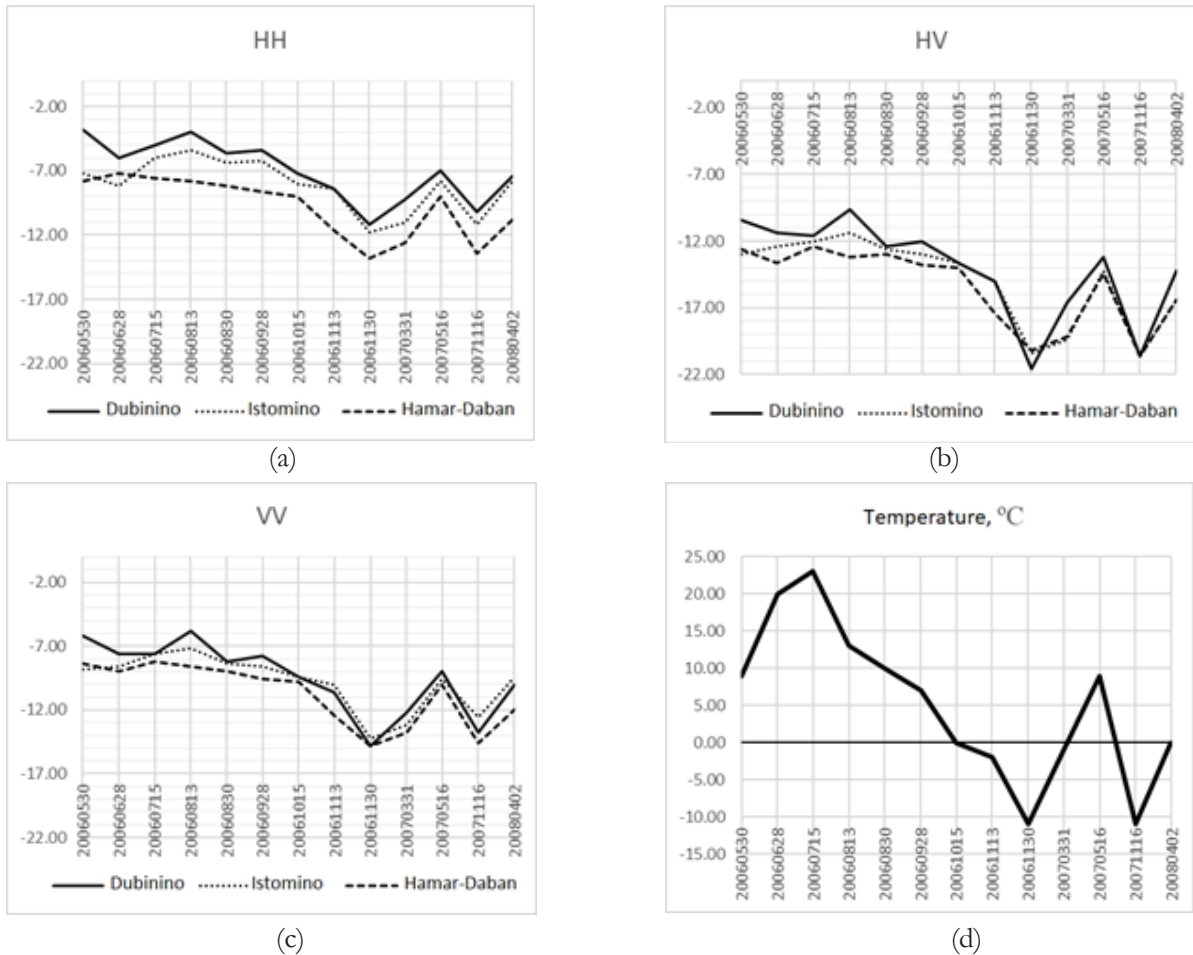


Fig. 1. Average NRCS (dB) of forest covers for different polarization combinations on receive/transmit (a – HH, b – HV, c – VV) and air temperature during observation (d).

November, in contrary to flatland test sites, where plots are alternation of maxima and minima. Mountainous forest shows the most significant response to zero crossing of air temperature: flatland forests' NRCS decreases by 0.4-1.4 dB between October 15 and November 13, 2006 (with air temperature 0°C and -2°C, respectively), the forest on mountain slopes shows NRCS decrease by 2.6 dB for co-polarized images and by 3.4 dB for cross polarization.

Pearson correlation coefficient for NRCS (in dB) with air temperature in the observation dates is rather high: its minimal value is 0.78 (Istomino forest, HH polarization), and its maximal value is 0.91 (mountainous forest, HH polarization). Air temperature influences on the scattering properties of trees indirectly, via change vegetation of moisture, and, hence, its dielectric constant. Aside from freezing in

an observation day, weather conditions of the precedent days are of importance: they cause drying, chilling and freezing processes in a bark of a tree and its inner layers. As L-band SAR signal can partially penetrate through vegetation and scatter from the ground, let us discuss non-forested test sites now in order to analyze soil's contribution to the forest backscatter later.

One can see also on the Fig. 1 that the minimal difference between NRCS lines for three forests is on VV polarization plot.

At first sight, the most obvious difference between forest (Fig. 1) and non-forest (Fig. 2) NRCS lines is a value spread in each date: NRCS difference for forests is less than 4 dB, while difference between some non-forest test sites reaches 14 dB. Besides, minima in frosty days are less explicit: although 5-7 dB alternations between winter and summer dates are visible for last four dates on all plots of

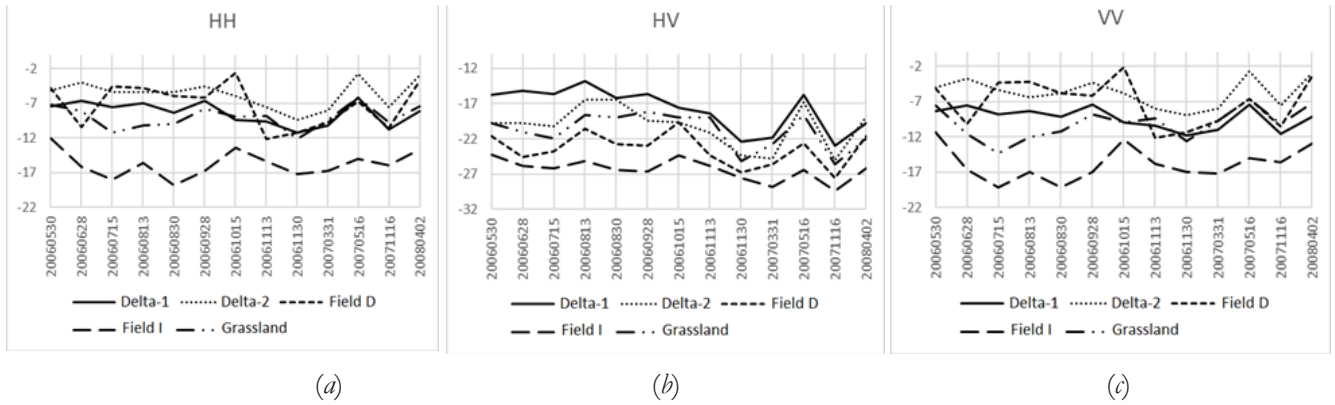


Fig. 2. Average NRCS (dB) of forest-free sites at: a) HH, b) HV, c) VV.

Fig. 2, difference between frosty November 30, 2016 (−11°C) and two surrounding days with air temperature −2°C and 0°C is not clear for the test sites. In general, correlation NRCS with air temperature is far less here: except for the Delta-1 test site with spots of shrub on it, Pearson correlation coefficient is between 0.2 and 0.6, and it has negative sign for some test sites. As for the Delta-1 test site, correlation is 0.8-0.86, which is close to forest values described above (0.78-0.92).

Two fields demonstrate near-chaotic lines on backscatter plots. It is related to the fact that the backscatter coefficient changes here prevalently due to cultivation of crops. Three non-cultivated test sites have moderate changes of NRCS, and are compatible to each other. Gradual NRCS decrease from August to November in 2006, which is evident for forests (Fig. 1), it is absent for non-forest test sites for HH and VV polarizations, but is slightly visible on cross-polarization. The maximal difference of NRCS for non-cultivated test sites one can

find on VV polarization (the difference reaches up to 10 dB, see Fig. 2c), in contrast to forest NRCS, where VV polarization shows the minimal variations (less than 2.8 dB, Fig. 1c).

4. POLARIMETRIC CLASSIFICATIONS AND THEIR DYNAMICS DURING THE YEAR

Measurements of scattering matrix allow the estimation of contribution of different scattering mechanisms in total backscatter. Fig. 3 presents contribution of three main scattering mechanisms in percent: surface scattering, volume scattering, and double-bounce scattering, which are calculated by Freeman method [13]. Total power P of scattering matrix

$$S = \begin{bmatrix} S_{HH} & S_{HV} \\ S_{VH} & S_{VV} \end{bmatrix},$$

calculated by

$$P = |S_{HH}|^2 + 2|S_{HV}|^2 + |S_{VV}|^2,$$

in this method is decomposed into three components

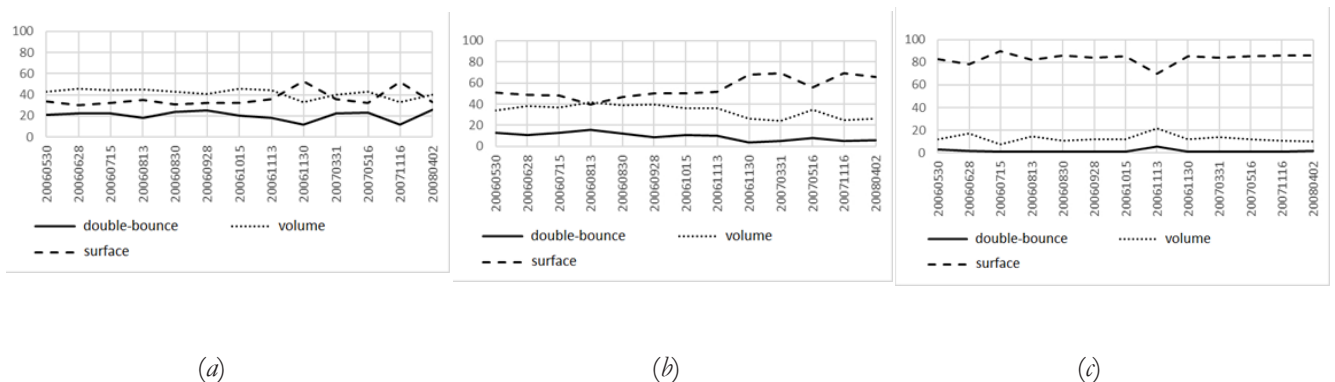


Fig. 3. Input of scattering mechanisms for forest D (a), forest-free site Delta-1 with presence of shrub (b), and Field D field (c).

$P = P_s + P_v + P_d$,
 where indices s , v and d denote surface, volume, and double-bounce scattering mechanisms, respectively.

Volume type of scattering dominates on Dubinino forest test site nearly always, except for the frosty dates. Graphs for other forests look similarly: volume scattering contribution is maximal (30%-47%) save for two frosty dates, the next mechanism is surface scattering, and double-bounce is the least significant scattering mechanism, but its contribution is far from being negligible (about 15-20% of total power). In frosty dates the most significant mechanism is surface scattering, its contribution becomes greater than 50% at the cost reducing two other mechanisms' contribution.

Surface scattering mechanism dominates in all the dates of observation of non-forested test sites (see Fig. 3b and 3c). Percent of double-bounce is lower in comparison with forests (3-16% on Delta-1 test site with shrubs in it, and 1-6% on fields). Volume scattering is in-between surface and double-bounce scattering for non-forested test sites for all the observation dates. However, on shrubby test site Delta-1 the volume scattering percent is comparable with the surface scattering (24-42% and 40-69%, respectively), and on fields volume scattering contribution is about one fifth of the surface one (8-22% and 70-90%).

An alter classification method for polarimetric data related to scattering mechanisms is a polarimetric decomposition by S.R. Cloude and E. Pottier [12], which is based on spectral analysis of coherency matrix. Using this method, one can estimate diversity of eigenvalues p_i of coherency matrix (this diversity is denoted as an entropy H):

$$H = -\sum_{i=1}^3 p_i \log_3 p_i, \quad p_i = \frac{\lambda_i}{\lambda_1 + \lambda_2 + \lambda_3}.$$

The second important parameter in this method is an angle α calculated as a weighted average of angles α_1 , α_2 and α_3 , which can be

calculated by parameterization of the first coordinate of eigenvectors of coherency matrix in the form of $\cos\alpha_i$. Values p_i are taken as weights for α_i :

$$\alpha = \sum_{i=1}^3 p_i \alpha_i.$$

Unlike the above-mentioned technique, where weighted input of each of three scattering mechanisms is evaluated for the area of interest, Cloude-Pottier decomposition identifies main scattering mechanism, which can be related to one of eight classes. The classes are characterized by level of parametric angle α and entropy H of eigenvalues of coherency matrix. Angle α values from the interval between 0° and 40° - 42° correspond to surface type of backscatter, from the interval between 40° - 42° and 50° - 55° — to dipole scattering, and above 55° — to double bounce backscatter. Surface scattering area in H - α plane consists of two classes: low entropy and moderate entropy, which is generally related to the rate of small-scale roughness of a scattering surface. Dipole scattering, which corresponds to volume scattering in Freeman decomposition, is subdivided in three classes (with low, moderate and high entropy). Double bounce scattering mechanism is subdivided similarly into three classes according to the entropy level.

In **Fig. 4** the angle α dynamics for all the observation dates and eight test sites is shown. Horizontal dashed lines mark levels 40° и 55° . The plots of this parameter for three forest sites marked here as 1, 2, and 3 are located between these levels except for the measurements made in two cold days and with near zero temperature at

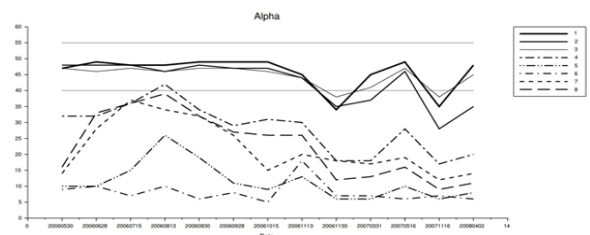


Fig. 4. Values of α angle for eight test sites.

Istomino test sites on March 31, 2007 and April 2, 2008. All the measurements over forest-free areas (lines 4-8) demonstrate surface scattering type except for the only observation on the date 20060813, Delta-1 test site, with some amount of shrub vegetation which has intermediate position in the classification scheme between fields and forests.

Entropy values are presented in **Fig. 5**. Forests (lines 1-3) shows the highest entropy, at the same time it never exceeds the threshold level 0.9, which subdivides surface scattering types with moderate and high entropy. In cold days the entropy of forests decreases and lies within the band of moderate values 0.5-0.9. Below the 0.5 value there are the measurements for two test sites – Delta-2 and Field D. Almost all the points of plot for the test site Delta-1 are in the area of moderate entropy; the entropy drops below 0.5 only in cold days and in the beginning of spring (March 2007 and April 2008). In the end of spring (May 2006 and May 2007) the entropy for this site is close to summer values. Other forest-free sites show low entropy in spring and winter, and moderate one in summer and autumn. It is worth noting that in this polarimetric classification scheme the H and α parameters are correlated in much extent in the case of observations of forest covers in L-band, since double bounce scattering effect is the least significant mechanism.

Combination of H and α values allows marking every image pixel by one of eight classes. Fig. 4 and 5 show that some graphs cut the threshold lines, it means that in different dates the classification scheme produces different results. An example of classification

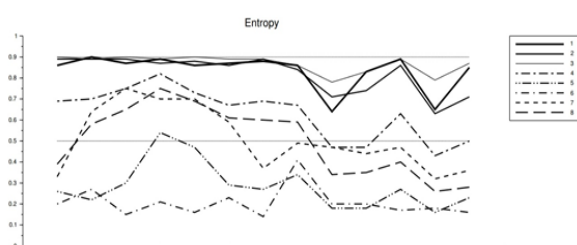


Fig. 5. Entropy values for eight test sites.

map one can see on the **Fig. 6**. In the left part of the figure there is result of classification of the data acquired on June 28, 2006 (air temperature $+20^{\circ}\text{C}$), and in the right half of the figure is a classification map for November 16, 2007 (air temperature 11°C below zero). Test sites are marked by rectangles: white one on the forest (“Forest D” on Fig. 1, 3-5), black one on the field (“Field D” on the Fig. 2-5).

The field test site on both classification maps on the Fig. 6 relates to the same class: surface scattering with low entropy. In the contrary, the forest site is shown as dipole-type scattering class in summer (light grey color with darker roads and rare bright double-bounce pixels), but in winter it moves to another class: grey moderate entropy surface scattering). As one can see on the Fig. 6, the same is true for the whole forest massive, except for a number of tiny spots: in winter the dipole class vanishes, and the double-bounce one is totally absent. Non-forested area in the left half of the Fig. 6a) and 6b) becomes the class of surface scattering with low entropy in winter (dark grey color).

Thus, Cloude-Pottier polarimetric classification doesn't guarantee reliable delineation of the forest (since in summer the dipole class contains not only forest pixels, it includes also a fragment of bushy river delta in the upper left corner of the Fig. 6a, and in

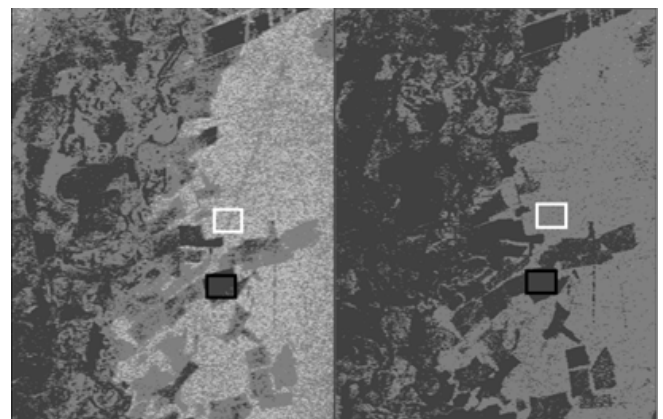


Fig. 6. Summer (a) and winter (b) classification results for Dubinino forest surroundings using Cloude-Pottier decomposition. White color: double-bounce scattering, light-gray: dipole scattering, gray: surface scattering with moderate entropy, dark-gray: surface scattering with low entropy.

winter a large amount of non-forested surfaces is in the same class with the forest on the Fig. 6b). But the combination of two classification maps from warm and cold days gives us a desired result: non-forested surfaces shows the surface type scattering on both classifications, forest is in dipole class in summer and medium entropy or dipole class in winter.

5. CONCLUSION

Radiophysical properties of such a natural covers as boreal forests are essentially dependent on measurement conditions, first of all, on air temperature. In cold season NRCS of vegetation drops for all SAR signal combinations of polarizations on transmit/receive. Cross polarization demonstrates the most significant decrease of NRCS, it reaches 12 dB here, whereas changes of co-polar NRCS are less than 7-8 dB. Application of decomposition methods for polarimetric SAR data taken in different season of year allows revealing difference in scattering mechanisms behavior for vegetated and bare soils. While the dominant mechanism in non-forested areas is surface scattering with moderate entropy throughout the year, a dipole scattering type in forests in summer is substituted by the surface scattering in winter. These special aspects of radiophysical properties of scattering covers affect the automatic classification methods and accuracy of measuring their structural and biophysical characteristics. At the same time, joint analysis of data acquired in warm and cold seasons enhances classification of earth covers

REFERENCES

1. Le Toan T, Beaudoin A, Riou J, and Guyon D. Relating forest biomass data. *IEEE Trans. on Geosci. and Remote Sensing*, 1992, 30(2):403-411.
2. Dobson MC, Ulaby FT, Le Toan T, Beaudoin A, Kasischke ES, Christensen N. Dependence of the radar backscatter on coniferous forest biomass. *IEEE Trans. on Geosci. and Remote Sensing*, 1992, 30(2):412-415.
3. Kurvonen L, Pulliainen J, and Hallikainen M. Retrieval of Biomass in Boreal Forests from Multitemporal ERS-1 and JERS-1 SAR Images. *IEEE Trans. on Geosci. and Remote Sensing*, 1999, 37(1):198-205.
4. Kwok R, Rignot EJM., Way J, Freeman A, and Holt J. Polarization Signals of Frozen & Thawed Forests of Varying Environmental State. *IEEE Trans. on Geosci. and Remote Sensing*, 1994, 32(2):371-381.
5. Ranson KJ, Sun G. Northern forest mapping biomass of a forest using multifrequency SAR data. *IEEE Trans. on Geosci. and Remote Sensing*, 1994, 32(2):388-396.
6. Pulliainen JT, Heiska K, Hyyppä J, Hallikainen MT. Backscattering properties of boreal forests at the C- and X-bands. *IEEE Trans. on Geosci. and Remote Sensing*, 1994, 32(5):1041-1050.
7. Armand NA, Zakharov AI, Kucheryavenkova IL. Issledovanie otrazhatelnykh kharakteristik lesov Podmoskov'ya po dannym SIR-C XRD [The study of the reflective characteristics of forests in the Moscow region according to the SIR-C XRD data]. *Radiotekhnika*, 1998, 9:27-31 (in Russ.).
8. Pulliainen JM, Hallikainen M.M. Feasibility of multitemporal interferometric SAR data for stand level estimation of boreal forest stem volume. *Remote Sensing of Environment*, 2003, 85(4):397-409.
9. Wollersheim M, Collins MJ, Leckie D. Estimating boreal forest species type with airborne polarimetric synthetic aperture radar. *Int. J. of Remote Sensing*, 2011, 32(9):2481-2505.
10. Cloude SR, Papathanassiou KP. Polarimetric SAR Interferometry. *IEEE Trans. on Geosci. and Remote Sensing*, 1998, 36(5):1551-1565.
11. Mette T, Papathanassiou KP, Hajnsek I, Zimmermann R. Forest Biomass Estimation using Polarimetric SAR Interferometry. *Proc. of Intl. Geosci. And Remote Sensing Symp.*

(Toronto, Canada, June 24-28, 2002), pp. 3859-3862.

12. Cloude SR and Pottier E. An Entropy Based Classification Scheme for Land Applications of Polarimetric SAR. *IEEE Trans. on Geosci. and Remote Sensing*, 1997, 35(1):68-78.
13. Freeman A and Durden SL. A Three-Component Scattering Model for Polarimetric SAR Data. *IEEE Trans. on Geosci. and Remote Sensing*, 1998, 36(3):963-973.